TETRAHEDRON FORMATION CONTROL[*]

José J. Guzmán[†]

a.i. solutions, Inc.
10001 Derekwood Lane, Suite 215, Lanham, MD 20706, USA

ABSTRACT

Spacecraft flying in tetrahedron formations are excellent instrument platforms for electromagnetic and plasma studies. A minimum of four spacecraft - to establish a volume - is required to study some of the key regions of a planetary magnetic field. The usefulness of the measurements recorded is strongly affected by the tetrahedron orbital evolution. This paper considers the preliminary development of a general optimization procedure for tetrahedron formation control. The maneuvers are assumed to be impulsive and a multi-stage optimization method is employed. The stages include targeting to a fixed tetrahedron orientation, rotating and translating the tetrahedron and/or varying the initial and final times. The number of impulsive maneuvers can also be varied. As the impulse locations and times change, new arcs are computed using a differential corrections scheme that varies the impulse magnitudes and directions. The result is a continuous trajectory with velocity discontinuities. The velocity discontinuities are then used to formulate the cost function. Direct optimization techniques are employed. The procedure is applied to the Magnetospheric Multiscale Mission (**MMS**) to compute preliminary formation control fuel requirements.

INTRODUCTION

This paper reports the results of a preliminary study on the development of a general optimization procedure for tetrahedron formation control. The methods employed, however, are general and could be applied to other types of formations. In general, for this type of "in-situ" mission maintaining a tight formation during the orbital evolution is not necessary. It is of importance, however, to maintain tetrahedron size and shape metrics (quality factors, see ref. 1) within "acceptable" values. Typically, this quality factor maximization can be achieved by a judicious choice of initial conditions. The formation then evolves naturally (without maneuvers) while collecting science data. In this investigation, the maneuvers needed to transfer the formation from its current configuration to the initial conditions at the beginning of the science arc are examined. In an effort to minimize fuel expenditure, a multi-stage optimization method is employed. The algorithms developed for this investigation do not make any assumptions on the location and number of burns that will be used. Direct optimization techniques that have been utilized previously are used (ref. 2). No claims are made about the global optimality of the solutions, only that the solutions computed are a local optima given the inputs and constraints. In fact, an experienced analyst might be able to take some of the resulting solutions and further improve them via numerical experimentation. Nevertheless, the ultimate goal is to automate the mission design process as much as possible by quickly computing solutions that are at least local minima. The methodology is applied to the NASA Goddard Magnetospheric Multiscale Mission to gain understanding about the fuel needed to perform certain tasks.

PREVIOUS WORK

A tetrahedron mission, Cluster II is currently flying and operating successfully (ref. 3). In the process of planning the Cluster mission, fuel optimization of the maneuvers needed to initialize, modify and maintain the formation was considered by J. Rodríguez-Canabal and M. Belló-Mora (ref. 4). Later a different optimization method was employed by J. Schoenmaekers (ref. 5). In J. Schoenmaekers's paper, both methods are compared for one mission scenario. Moreover, a further-developed strategy is presented by M. Belló-Mora

---

[†]Aerospace Engineer, Mission Analysis Department, a.i. solutions, Inc.

and Rodríguez-Canabal (ref. 6). Implementation and operational results for the maneuvers are reported by D. Hockens and J. Schoenmaekers (ref. 7). These Cluster references provide a solid foundation for the work in the current investigation.

In this paper the mission of interest is the MMS Mission (ref. 8). MMS will determine the small-scale basic plasma processes which transport, accelerate and energize plasmas in thin boundary and current layers. These processes control the structure and dynamics of the Earth's magnetosphere. For the interested reader, preliminary mission design and analysis for MMS, which includes a double lunar swingby for one of its phases, has been presented by: A. Edery and C. Schiff (ref. 9), A. Edery (ref. 10), J. Guzmán and A. Edery (ref. 11), C. Petruzzo (ref. 12), and S. Hughes (ref. 13). Furthermore, at some point tetrahedron formations might be used to study the magnetic field of other bodies in our solar system.

APPROACH

For the purpose of this investigation we will divide the formation flying design into two distinct arcs. The first arc includes a sequence of maneuvers that transfers the formation from its current configuration (position and velocity states) to a configuration appropriate for the start of the second arc, the science one. In this paper, the formation configuration at the beginning of the science arc is called the target configuration. See Figure 1. Note that the science arc does not contain any maneuvers. In fact, the absence of maneuvers benefits the science data gathering by limiting the orbital disturbances. The two arcs then lead to two coupled optimization problems: (1) compute the initial states of the science arc that maximize a certain tetrahedron quality factor along the science arc, and (2) compute the maneuver sequence that minimizes the fuel needed to transfer the formation from its current configuration to the target configuration. In this paper, only the second problem is considered. In refs. 12, 13 the first problem is considered. Since the two problems are coupled, the goal is to eventually merge these two optimization processes. For now a target configuration is assumed to develop algorithms that solve the second problem. In other words, the four states that comprise the target configuration are considered as given for the maneuver optimization process. Nevertheless, tetrahedron rotations and translations are allowed in the target configuration in order to further lower the fuel consumption (these changes might not be possible when the two problems are solved simultaneously).
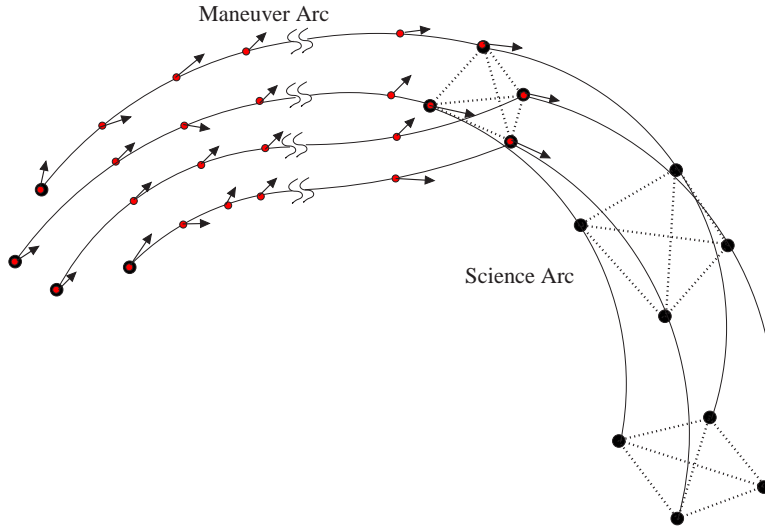

Figure 1: Maneuver and Science Arcs

The Concept of a Reference Path

The trajectory design strategy for MMS involves obtaining a reference or nominal path that traverses the magnetospheric regions of interest. Relative to this defined reference path, a tetrahedron formation is established at certain times during the mission. Those times will be specified by the scientists. The science mission consists of four phases: the first two phases traverse regions of the magnetosphere close to the magnetic equatorial plane, the third phase contains a double lunar swingby sequence (**DLS**) with an investigation of the deep tail magnetospheric region, and the fourth phase explores regions perpendicular to the ecliptic. The different MMS phases and their corresponding scientific goals are explained by S. Curtis (ref. 8). The science goals, in turn, help to specify the orbital requirements for each phase. The main orbital requirements are shown in Table 1 (ref. 8). It is likely that some flexibility in the location of the formation relative to the reference path might be allowed (if the magnetospheric regions of interest are still traversed by the formation). Furthermore, the reference trajectory could be redefined. Still, since one of the phases includes a double lunar swingby, monitoring the formation relative to the reference path is of interest.[1]

Table 1: MMS Reference Path Orbital Requirements

Mission Phase	Perigee $(R_\oplus)$	Apogee $(R_\oplus)$	Semi-Major Axis (km)	Eccentricity	Inclination (degrees)
Phase 0	1.2	12	42,094	0.818	28.5*
Phase 1	1.2	12	42,094	0.818	10*
Phase 2	1.2	30	99,496	0.923	10-20*
Phase 3	N/A	> 100	N/A	N/A	N/A
Phase 4	10	50	191,340	0.666	90**

* Equatorial Inclination, ** Ecliptic Inclination

Coordinate Systems

For the purpose of this investigation, three orthogonal Cartesian coordinate systems are employed. The first system is the inertial Mean of J2000 coordinate frame. The second frame utilizes the reference path orbital velocity, binormal and normal directions (**VBN**). The third frame is introduced to consider tetrahedron translation and rotations. It is placed at the tetrahedron centroid and it is initially coincident with the second frame. See Figure 2. Table 2 summarizes the frames employed (and their respective origins) and introduces the unit vector notation used in Figure 2.
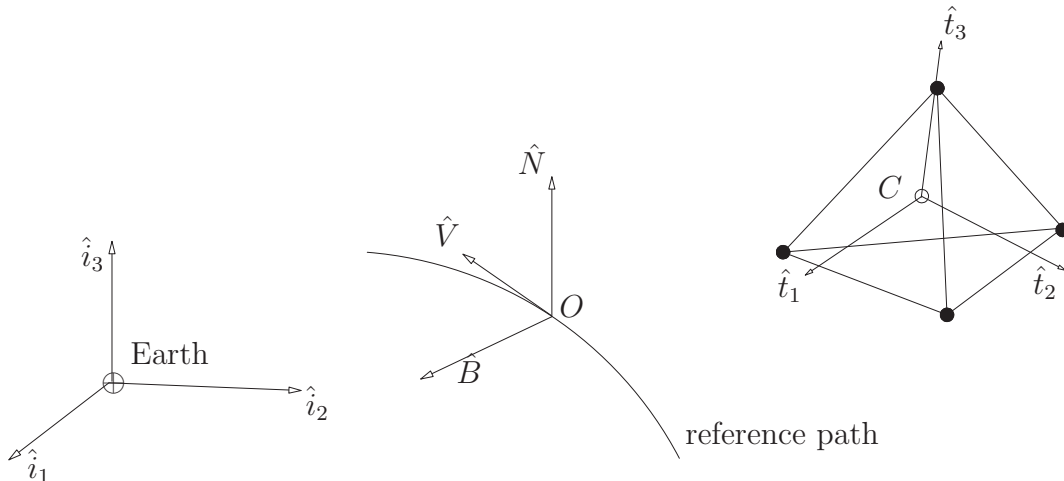

Figure 2: MMS Frames

---

[1] Because the timing provided by the reference path is important for the lunar encounters.

Table 2: Coordinate Frames

Type	Unit Vectors	Origin
Inertial	$(\hat{i}_1, \hat{i}_2, \hat{i}_3)$	$\oplus$ - Earth's center
Rotating	$(\hat{V}, \hat{B}, \hat{N})$	O - Reference spacecraft (fictitious)
Rotating	$(\hat{t}_1, \hat{t}_2, \hat{t}_3)$	C - Tetrahedron centroid

Initial Conditions for the Science Arc

The algorithms developed for this study are independent of the initial states selected for the science arc; yet the actual computations depend on them. In this section, a method to select the targets states at the beginning of the science arc is explained (other choices are possible). A regular tetrahedron[2] is used to meet the science data collection requirements. A reference orbit is specified and the individual spacecraft locations are set using spherical coordinates in the VBN frame (ref. 15). The velocity direction is kept the same as that of the reference orbit, i.e. the VBN frame velocity direction.[3] Then, the velocity magnitude is obtained using the two-body problem energy or vis-viva equation, thus, $v = \sqrt{\mu\left(2/r - 1/a\right)}$, where v is the velocity magnitude, r is the position magnitude (radial distance), μ is the gravitational parameter and a is the semi-major axis. Changing the velocity directions in order to maximize a certain tetrahedron quality factor has been investigated by C. Petruzzo (ref. 12). The investigation has been extended by S. Hughes (ref. 13) to consider both the initial positions and velocities.

Initial Guess for the Maneuver Sequence

The first step in optimizing a particular problem is to obtain an initial guess. In this case we obtain an initial guess by propagating from some initial configuration. The initial states for the maneuver arc are also specified as explained in the *Initial Conditions for the Science Arc* section. (This specification is for computational convenience. During spacecraft operations the states would be set by the formation configuration at the specified start time for the maneuver arc). Then, the reference and the four spacecraft formation are propagated without any maneuvers. While propagating, discrete states along the path are saved. The discretization interval is selected by the user. In this case, a discretization in terms of true anomaly (**TA**) along the reference path is utilized. See Figure 3 for TA discretizations of 180, 90, 45 and 22.5 degrees. These TA discretizations provide 3, 5, 9, and 17 patch states respectively. These discrete states (**"patch states"**) are states where maneuvers might be implemented. It is important to realize that a spacecraft path with, for example, 17 maneuvers will not be implemented in practice. Nevertheless, numerically implementing such a path will show the best locations to perform the maneuvers. (Furthermore, many of the resulting maneuvers are "small" and can be eliminated and/or combined. As a result, the analyst can compute operationally feasible solutions).
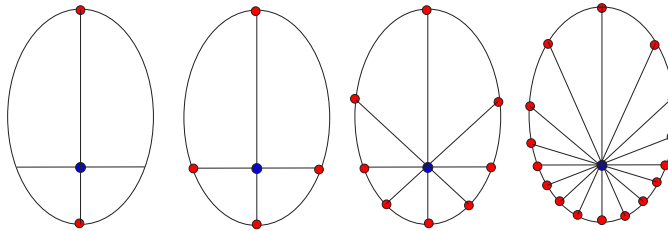

Figure 3: True Anomaly Discretization: Initial Maneuver Locations

---

[2]A regular tetrahedron is useful in cases where sampling of the structure of a field is not as important as understanding its transient or fluctuating events (ref. 14).

[3]This assumption is adequate when the spacecraft-to-reference separation is "small" relative to the reference-to-Earth separation.

Computing the Optimal Maneuver Sequence

Once the initial and final states have been set for the maneuver sequence, the target/optimization process can proceed. The optimization approach involves combining the fuel optimization of each spacecraft with the minimization of the total fuel usage to achieve a target configuration. The total fuel usage is the sum of the totals for each of the four spacecraft ($\mathbf{S/C}$). In terms of the spacecraft engine, only impulsive maneuvers are considered (thus only velocity change or $\mathbf{\Delta V}$ numbers are presented). For computational speed purposes, the optimization is performed sequentially in two stages: (1) each spacecraft trajectory is optimized by minimizing the fuel used by each spacecraft to achieve its target location in the tetrahedron, then, (2) the final tetrahedron configuration is varied (translated and rotated relative to some arbitrary configuration in the vicinity of the reference path) while minimizing the sum of all the spacecraft ΔVs. Better results might be obtained by completely embedding step (1) in each iteration of step (2). Nevertheless, if the target orientation is specified by the scientific requirements and/or by the optimization of a certain quality factor, step (2) might not be allowed. For both stages, as the impulse locations and times change (i.e., as the initial TA discretizations in Figure 3 change), new arcs are computed using a differential corrections (targeting) scheme that varies the impulse magnitudes and directions.

In the first optimization stage and for each spacecraft, the transfer trajectory problem becomes essentially a rendezvous problem. The techniques introduced in ref. 2 are employed. Each spacecraft path is discretized into a set of n patch states. The independent variables chosen are the changes in the internal and final patch state locations and times (i.e., four independent variables at each patch state). Thus, there are $4 \times (n-1)$ independent variables per spacecraft. For numerical purposes, the changes are constrained to stay within some user defined limits. Each spacecraft trajectory is optimized independently using the total ΔV as the cost function. The optimization method selected is the Sequential Quadratic Method (SQP).

In the second optimization stage, the target tetrahedron is allowed to translate within some limits and to rotate about its centroid. The sum of all the spacecraft ΔVs is the cost function. The optimization method selected for the second stage is a Genetic Algorithm (GA) that varies 6 independent variables (3 variables for the translation and 3 variables for the rotation). For this preliminary investigation, following some empirically developed guidelines (ref. 16), a population size of $N = 4b$, where b is the number of bits in the binary chromosome, and a mutation probability of $P_{\mathrm{mut}} = (b+1)/2Nb$ were utilized. The setup for the GA is still under investigation.

SOME RESULTS FOR MMS

The methodology described in this paper is applied to the MMS mission. The reference orbital states considered are consistent with the orbit requirements of MMS (see Table 1). At the end of the maneuver arc, the maximum errors allowed for each spacecraft position and time are 10% of the desired inter-spacecraft distance and 0.5 seconds respectively. Although the algorithms developed for this study are independent of the particulars of the force model and integrator, the actual computations depend on them. The dynamical model that is adopted to represent the forces on the spacecraft includes the gravitational influences of the Sun, Earth, Moon and Jupiter (obtained from the Jet Propulsion Laboratory Definitive Ephemeris 405 file). Solar radiation pressure (flat plate model) and the Earth's J_2 Earth gravity harmonic are also included. For the numerical integration scheme, a Runge-Kutta-Verner 8(9) integrator is utilized. Next, some results are presented for each mission phase.

Phases 1 and 2

As a test, different cases (with 3, 5, 9, and 17 maneuvers per spacecraft) are examined *for one orbit.* (The initial states are specified at the apogee of the reference orbit and the target states are at the next apogee). For both Phases, three initial and three final tetrahedron sizes (inter-spacecraft separations between each spacecraft) are considered: 10, 1000, and 2000 km. When the initial and final sizes are the same, the problem is a maintenance problem; otherwise, it is a re-sizing problem. The results for Phase 1 are in Table 4 and the results for Phase 2 are in Table 5. Note that the cost associated with Phase 1 is higher than for Phase 2. This result can be explained by the fact that Phase 1 has a smaller apogee and thus a larger J_2 perturbation. However, a more extensive analysis should be performed to understand the different perturbation effects on

the tetrahedron evolution during the different orbital phases. While computing some of these test cases, it was observed that the tetrahedron translation and rotations did not help to lower the total ΔV in the one-orbit maintenance cases. This fact is not surprising given the fact that only one orbit was considered and the perturbation effects did not cause the formation to rotate much. It is observed that cases such as a 10 to 1000 km and 1000 to 10 km have similar — but not quite the same — costs. This result can be explained by examining the requested formation changes in terms of the individual spacecraft orbital elements. Note that some cases did not "converge". This label means that either the targeter could not meet the requested tolerance or that the ΔV computed was too "high". It is possible to further examine and perhaps "fix" these cases one by one. Specifically, one could change the tolerances; increase the maximum number of iterations allowed, etc. However, at this moment interest is in automation and speed.

Phase 3

In Phase 3, the formation will traverse the deep tail of the magnetosphere during a double lunar swingby sequence. At this point, there is no plan to perform any deterministic maneuvers for formation flying. That is, the final maneuver at perigee before the first lunar swingby produces a trajectory that requires no further maneuvers until Phase 4 begins after the second swingby. Thus, the formation will evolve under its natural dynamics in the perturbed Sun-Earth-Moon system. Non-deterministic maneuvers, however, will be used for any needed corrections.

Phase 4

After the double lunar swingby sequence, it is of interest to know how much fuel would be required to restore the tetrahedron at the next apogee. In ref. 11, three maneuvers (after the double lunar swingby) were used to restore the tetrahedron at the target apogee: the maneuver at perigee, an additional maneuver at the semi-latus rectum radial distance (this location was just an initial guess), and a maneuver at the target apogee. The lowest ΔV cost computed was for an initial separation of 10 km at the beginning of Phase 3 and a target separation of 200 km at the apogee after the double lunar swingby. The ΔV results in ref. 11 were higher because each spacecraft was constrained to be at its own apogee at the end of the sequence. In this investigation, only the reference spacecraft is at its apogee at the target time. Furthermore, as explained earlier in this section, errors in the final locations and times are allowed. The following results are obtained for 5 maneuvers (per spacecraft): 1.078 m/s for S/C 1, 0.812 m/s for S/C 2, 1.107 m/s for S/C 3 and 0.532 m/s for S/C 4. See Table 6 for more results. It should be remarked that these tables are different from the Phases 1 and 2 Tables since the start of the maneuver sequence is at perigee. Thus, the formation traverses only half of the reference orbit. Furthermore, the formation was initialized before the DLS (at the start of Phase 3). Therefore, the start of the maneuver sequence is at the perigee after the DLS and the formation is not in a regular tetrahedron but in some elongated shape with an average inter-spacecraft distance of 24 km.

MMS FUEL BUDGET IMPLICATIONS

Following some of the preliminary ideas in ref. 8, a mission scenario with the following formation re-sizings can be constructed:

- Phase 1: 1000 → 10 → 1000 → 10 km
- Phase 2: 10 → 2000 → 1000 → 2000 km
- Phase 3: N/A
- Phase 4: Reform with inter-spacecraft distance of 2000 km.

Then, the preliminary fuel requirements displayed in Table 3 can be computed. In this table, many items are still to be determined (**TBD**). Note also that the fuel cost in this table does not include error corrections, attitude, and other maneuvers. The budget allocated in ref. 8 is about 1000 m/s, therefore, the science team must iterate with the flight dynamics team on the desired formation flying requirements.

Table 3: ΔV (Per S/C) for Scenario in Ref. 8

Event or Phase	ΔV [m/s]
Phase 0 to Phase 1	326
Initializing the formation	TBD
Formation Re-sizing Phase 1	140
Formation Maintenance Phase 1	TBD
Phase 1 to Phase 2	277
Formation Re-sizing Phase 2	60
Formation Maintenance Phase 2	TBD
Phase 2 to Phase 3 to Phase 4	150
Formation Re-Configuration Phase 4	10
Formation Re-sizing Phase 4	TBD
Formation Maintenance Phase 4	TBD
TOTAL (adding currently available)	963 $\pm$ TBD

FURTHER FUEL COST REDUCTION

Further reduction in the fuel cost can be obtained by running the optimization stages completely nested. That is, for each new target orientation compute the optimal trajectories for each spacecraft. This process requires more computational resources but can be done with selected cases. Other resources include, but are not limited to: (a) varying the final (target) time, (b) establishing the tetrahedron relative to one of the four spacecraft (thus, one spacecraft is not required to maneuver), (c) allowing several orbit revolutions before performing any maneuvers (e.g. maintenance), etc. In option (b), the analyst should check that deviations from the desired reference path do not have adverse science and trajectory effects. Additional insight is obtained by looking at the required configuration changes in terms of the orbital elements. This insight might lead the analyst to lower cost solutions. In fact, by computing the orbital elements, it can be shown that formation re-sizings require mostly line of nodes and line of apsides changes.

SUMMARY

In this paper the problem of maneuvering a tetrahedron formation while minimizing fuel expenditure is considered. The optimization is performed sequentially in two stages: (1) each spacecraft trajectory is optimized by minimizing the fuel used by each spacecraft to achieve its target location in the tetrahedron, then, (2) the final tetrahedron configuration is varied (translated and rotated relative to some arbitrary configuration in the vicinity of the reference path) while minimizing the sum of all the spacecraft ΔVs. The methodology is applied to the NASA Goddard Magnetospheric Multiscale Mission to gain understanding about the fuel needed to perform certain tasks. No claims are made about the global optimality of the solutions; only that the solutions computed are a local optima given the inputs and constraints. Nonetheless, the ultimate goal is to automate the mission design process as much as possible by quickly computing solutions that are at least local minima. Future work includes the simultaneous optimization of the maneuver and science arcs, the application of the methodology to different mission scenarios, the inclusion of operational considerations/constraints and the integration of the developed software into the NASA Goddard mission analysis tools.

REFERENCES

[1] J.J. Guzmán and C. Schiff. A Preliminary Study for a Tetrahedron Formation: Quality Factors and Visualization. In *AIAA/AAS Astrodynamics Specialists Conference*, Monterey, California, August 4-8 2002. AIAA 02-4637.

[2] S.P. Hughes, L.M. Mailhe, and J.J. Guzmán. A Comparison of Trajectory Optimization Methods for the Impulsive Minimum Fuel Rendezvous Problem. In *26th Annual AAS Guidance and Control Conference*, Breckenridge, Colorado, February 5-9 2003. AAS 03-006.

[3] R. Mugellesi-Dow, J. Dow, and G. Gienger. Cluster II: From Launch to First Constellation. In *16th International Symposium on Space Flight Dynamics*, Pasadena, California, December 2001.

[4] J. Rodríguez-Canabal and M. Belló-Mora. Cluster: Consolidated Report on Mission Analysis. Technical report, European Space Operation Centre, Darmstadt, Germany, July 1990. ESOC CL-ESC-RP-0001.

[5] J. Schoenmaekers. Cluster: Fuel Optimum Spacecraft Formation Control. In *ESA Symposium on Space Flight Dynamics*, pages 419–425, Darmstadt, Germany, December 1991. European Space Agency. SP-326.

[6] M. Belló-Mora and J. Rodríguez-Canabal. On the 3-d Configurations of the Cluster Mission. In *ESA Symposium on Space Flight Dynamics*, pages 471–479, Darmstadt, Germany, December 1991. European Space Agency. SP-326.

[7] D. Hocken and J. Schoenmaekers. Optimization of Cluster Constellation Manoeuvres. In *16th International Symposium on Space Flight Dynamics*, Pasadena, California, December 2001.

[8] S.A. Curtis. The Magnetospheric Multiscale Mission...Resolving Fundamental Processes in Space Plasmas. NASA Goddard Space Flight Center, Greenbelt, Maryland, December 1999. NASA/TM—2000-209883.

[9] A. Edery and C. Schiff. The Double Lunar Swingby of the MMS Mission. In *16th International Symposium on Space Flight Dynamics*, Pasadena, California, December 2001.

[10] A. Edery. Designing Phase 2 for the Double-Lunar Swingby of the Magnetospheric Multiscale Mission (MMS). In *13th Space Flight Mechanics Meeting*, Ponce, Puerto Rico, February 9-13 2003. AAS 03-245.

[11] J.J. Guzmán and A. Edery. Flying a Four-Spacecraft Formation by the Moon...Twice. In *13th Space Flight Mechanics Meeting*, Ponce, Puerto Rico, February 9-13 2003. AAS 03-132.

[12] S.A. Curtis, C. Petruzzo, P.E. Clark, and A. Peterson. The Magnetospheric Multi-Scale Mission: An Electronically Tethered Constellation of Four Spacecraft. In *3rd International Workshop on Satellite Constellations and Formation Flying*, Pisa, Italy, February 24-26 2003. International Astronautical Federation.

[13] S. Hughes. Formation Tetrahedron Design for Phase 1 of the Magnetospheric Multi-Scale Mission. In *GSFC Flight Mechanics Symposium*, Greenbelt, Maryland, October 28-30 2003. NASA Goddard Space Flight Center.

[14] P. Robert, A. Roux, C.C. Harvey, M.W. Dunlop, P.W. Daly, and K.H. Glassmeier. Tetrahedron Geometric Factors. In G. Paschmann and P.W. Daly, editors, *Analysis Methods for Multi-Spacecraft Data*, pages 323–348. ISSI Report SR-001, ESA Publications Division, Noordwijk, The Netherlands, 1998.

[15] C. Schiff, D. Rohrbaugh, and J. Bristow. Formation Flying in Elliptical Orbits. In *2000 IEEE Aerospace Conference*, Big Sky, Montana, April 18-25 2000. Paper 317.

[16] E.A. Williams and W.A. Crossley. Empirically-Derived Population Size and Mutation Rate Guidelines for a Genetic Algorithm with Uniform Crossover. In P.K. Chawdhry, R. Roy, and R.K. Pant, editors, *Soft Computing in Engineering Design and Manufacturing*, pages 163–172. Springer-Verlag, 1998.

Table 4: ΔV Cost for Different Cases in Phase 1

Impulses per S/C	ΔV_{SC1}	ΔV_{SC2}	ΔV_{SC3}	ΔV_{SC4}	ΔV_{TOTAL} [m/s]
10 to 10 km					
3	0.253	0.235	0.077	0.187	0.752
5	**0.028**	**0.023**	**0.010**	**0.022**	**0.084**
9	0.029	0.029	0.031	0.026	0.115
17	0.042	0.036	0.046	0.032	0.156
10 to 1000 km					
3	41.117	58.301	66.300	*	N/A
5	39.042	52.567	59.247	56.586	207.442
9	**42.195**	**47.223**	**60.079**	**32.298**	**181.795**
17	67.829	47.910	39.409	68.365	223.512
10 to 2000 km					
3	82.772	116.749	132.839	*	N/A
5	69.385	120.594	93.236	126.301	409.516
9	**77.264**	**61.698**	**148.880**	**74.064**	**361.906**
17	78.616	146.109	144.089	74.454	443.269
1000 to 10 km					
3	39.749	58.320	69.079	*	N/A
5	38.584	52.718	59.994	56.589	207.885
9	**35.835**	**50.819**	**58.251**	**44.049**	**188.954**
17	39.184	62.433	69.373	60.850	231.840
1000 to 1000 km					
3	0.508	0.592	1.275	0.081	2.457
5	**0.420**	**0.554**	**1.231**	**0.088**	**2.293**
9	0.415	0.563	1.219	0.102	2.299
17	0.616	0.754	1.706	0.114	3.189
1000 to 2000 km					
3	41.205	55.613	66.832	*	N/A
5	39.723	51.590	59.229	57.785	208.327
9	**36.540**	**49.710**	**58.098**	**44.388**	**188.736**
17	40.016	61.444	68.990	61.490	231.939
2000 to 10 km					
3	78.732	115.462	144.820	*	N/A
5	77.412	104.583	121.030	114.301	417.326
9	**71.936**	**101.521**	**118.155**	**88.540**	**380.153**
17	78.758	125.638	139.962	122.593	466.950
2000 to 1000 km					
3	38.559	45.998	71.591	*	N/A
5	38.514	52.814	62.622	57.765	211.715
9	**35.859**	**51.287**	**60.888**	**44.602**	**192.637**
17	39.317	63.586	71.842	61.705	236.450
2000 to 2000 km					
3	0.914	1.097	3.186	0.154	5.351
5	0.814	1.078	2.870	0.173	4.936
9	**0.772**	**1.074**	**2.829**	**0.179**	**4.853**
17	1.149	1.433	3.955	0.189	6.726

* did not converge

Table 5: ΔV Cost for Different Cases in Phase 2

Impulses per S/C	ΔV_{SC1}	ΔV_{SC2}	ΔV_{SC3}	ΔV_{SC4}	ΔV_{TOTAL} [m/s]
10 to 10 km					
3	0.076	0.043	0.011	0.024	0.153
5	**0.025**	**0.022**	**0.022**	**0.023**	**0.092**
9	0.026	0.027	0.028	0.025	0.105
17	0.037	0.037	0.040	0.037	0.151
10 to 1000 km					
3	17.491	23.479	23.479	*	N/A
5	15.203	19.530	20.617	21.954	77.304
9	12.794	15.701	19.958	8.847	57.300
17	**24.324**	**9.329**	**10.069**	**13.354**	**57.077**
10 to 2000 km					
3	35.130	46.833	46.612	*	N/A
5	45.762	44.764	32.428	28.986	151.940
9	**21.847**	**23.541**	**52.335**	**16.014**	**113.738**
17	21.790	44.021	16.849	31.597	114.257
1000 to 10 km					
3	17.165	23.630	27.834	*	N/A
5	14.823	19.980	21.078	22.037	77.918
9	12.349	16.424	19.565	12.669	61.008
17	**11.149**	**16.599**	**20.483**	**12.704**	**60.936**
1000 to 1000 km					
3	0.496	1.018	1.139	0.308	2.962
5	0.453	0.432	0.989	0.250	2.124
9	0.302	0.337	0.707	0.216	1.563
17	**0.274**	**0.340**	**0.688**	**0.216**	**1.518**
1000 to 2000 km					
3	18.440	22.728	23.067	*	N/A
5	15.613	19.066	20.522	22.293	77.494
9	**12.783**	**15.889**	**19.450**	**12.596**	**60.718**
17	16.976	17.150	16.283	22.126	72.534
2000 to 10 km					
3	78.732	115.462	144.820	*	N/A
5	30.032	39.156	43.167	44.310	156.664
9	24.644	32.582	40.185	25.438	122.848
17	**22.281**	**33.145**	**41.822**	**25.498**	**122.745**
2000 to 1000 km					
3	14.441	37.554	42.702	*	N/A
5	14.772	19.935	22.848	22.391	79.945
9	12.192	16.666	20.923	12.902	62.682
17	**11.007**	**16.854**	**21.711**	**12.933**	**62.505**
2000 to 2000 km					
3	1.003	1.265	3.331	0.655	6.253
5	0.867	0.803	2.274	0.482	4.426
9	0.563	0.621	1.607	0.407	3.198
17	**0.492**	**0.612**	**1.575**	**0.395**	**3.073**

* did not converge

Table 6: ΔV Cost for Restoring the Tetrahedron in Phase 4

Impulses per S/C	ΔV_{SC1}	ΔV_{SC2}	ΔV_{SC3}	ΔV_{SC4}	$\Delta V_{\mathrm{TOTAL}}$ [m/s]
24 (avg.) to 200 km					
3	1.260	0.393	0.866	1.104	3.623
5	**1.078**	**0.812**	**1.107**	**0.532**	**3.530**
9	1.141	1.083	1.358	1.584	5.166
24 (avg.) to 1000 km					
3	**3.599**	**4.309**	**4.985**	**4.907**	**17.799**
5	3.824	4.862	5.330	4.911	18.927
9	7.564	7.948	6.287	5.777	27.577
24 (avg.) to 2000 km					
3	**6.343**	**10.917**	**10.537**	**9.307**	**37.104**
5	14.135	5.406	8.666	10.860	39.066
9	13.731	12.688	19.284	12.388	58.092